Energy Proceedings
Vol 36, 2023
ISSN 2004-2965

Anaerobic oxidation of methane with conditions of increased temperature and extra sulfate supply

Jianzhen Liang[1], Jing-Chun Feng[1,2*], Si Zhang[2,3], Cun Li[3]

1 School of Ecology, Environmental, and Resources, Guangdong University of Technology, Guangzhou 510006, China

2 Southern Marine Science and Engineering Guangdong Laboratory (Guangzhou), Guangzhou 511458, China

3 South China Sea Institute of Oceanology, Chinese Academy of Sciences, Guangzhou 510301, China

(*Corresponding Author: Jing-Chun Feng, fengjc@gdut.edu.cn)

ABSTRACT

Anaerobic oxidation of methane (AOM) coupled with sulfate reduction (SR) is an important process in cold-seep ecosystems to prevent methane emitted from the seafloor to the atmosphere. However, how the temperature and sulfate in seep habitats drive the SR-AOM process and further affect the methane cycles remains unknown. We simulated the habitat differences in sulfate and temperature using a high-pressure bioreactor system with a fed-batch mode for in vitro incubation of seep sediment. We found that SR-AOM was significantly affected by increased temperature (15°C). The AOM activity was increased by sulfate supply (+15 mM), even at a low temperature (8°C). Our findings provide a new insight into the methane budget in cold seeps.

Keywords: Cold seep, Anaerobic oxidation of methane, Sulfate, Temperature, Sediment incubation.

NONMENCLATURE

Abbreviations	
AOM	Anaerobic oxidation of methane
SR	Sulfate reduction

1. INTRODUCTION

Methane (CH_4) is an important greenhouse gas that produces more radiation per molecule of CH_4 than CO_2, making it more harmful to global warming [1]. The seafloor at continental margins contains large reservoirs of methane, where methane typically exists in solid gas hydrate, dissolved, and gaseous forms due to environmental differences [2]. Methane fluids within the reservoirs migrate from the subsurface into the water column through geologic processes, resulting in a process of methane seeping that may eventually even reach the atmosphere [3]. It is estimated that methane seeps globally emit 0.01-0.05 Gt of carbon to the atmosphere annually, accounting for 1-5% of global atmospheric methane emissions [4]. This suggests that methane seepage would be the dominant source of marine methane emissions.

AOM has been widely recognized as an effective global methane sink, preventing the escape of methane into the atmosphere from sediments [5, 6]. In marine sediments, methane is anaerobically oxidized by a consortium of anaerobic methanotrophic (ANME) archaea and sulfate-reducing bacteria using sulfate as the terminal electron acceptor [7]. AOM coupled with sulfate reduction consumes 90% of the methane produced in the sediments and 70% of the sulfate diffused into the sediments [8]. The SR-AOM process acts as an effective methane barrier, minimizing the released methane escape into the atmosphere [9]. The efficiency of AOM is affected by natural factors such as changes in temperature and sulfate concentration [10, 11]. However, limited investigations of AOM activity have been conducted due to the technical challenges of in situ monitoring of highly unstable environments. The exact AOM rate variations in distinct habitats with different temperatures and sulfate concentrations remain unrevealed.

In this work, we used a high-pressure bioreactor system with a fed-batch mode for in vitro incubation of seep sediment to simulate the habitat differences in sulfate concentrations and temperatures. Essentially, during the operation of this system, we independently

This is a paper for the 9th Applied Energy Symposium: Low Carbon Cities and Urban Energy Systems (CUE2023), Sep. 2-7, 2023, Matsue & Tokyo, Japan.

controlled temperature and sulfate concentration to simulate the AOM processes under different habitat conditions. The AOM activity and geochemical process were closely monitored during the experiment. Here, we illustrate the ecological impacts on AOM activity and geochemical processes.

2. MATERIAL AND METHODS

2.1 Sources of the sediment samples

Sediment samples from the Haima cold seep area located on the northern continental slope (South China Sea, 1384 m water depth). Surface sediment samples in the area were collected from the seafloor to the "Kexue" expedition vessel by using a box corer (30 cm deep) that contained pieces of gas hydrate (0.5–5 cm long). For subsequent experiments, sediment samples were collected only in the surface 0–5 cm of the box sample and then immediately stored at 4°C in sterile sample bags under a nitrogen atmosphere.

2.2 Scheme of the high-pressure bioreactor system

The high-pressure bioreactor system includes five main parts: the high-pressure bioreactor, the thermostatic water tank, the pump for injecting liquids, the monitor for temperature and pressure, the gas pressurization system, and the methane cylinder. In addition, the high-pressure sampler is used to maintain pressure and better separate the gas and liquid samples collected from the system.

The bioreactor has a volume of 1.67 L and is made of T316 stainless steel to prevent potential microbial corrosion. The bioreactor is placed in the thermostatic water tank (-15–80°C) to control the incubation temperature. The prepared basal medium is injected into the system using the pump for injecting liquids. The pressure inside this incubation vessel can be raised up to 16 MPa and is monitored by a pressure sensor. Methane in a gas cylinder is pumped into the bioreactor system via the gas pressurization system. The high-pressure methane gas provides pressure to the reactor system and acts as the headspace layer. By using the high-pressure sampler to connect to the system, the samples of gas, seawater, sediment, and pore water can be collected.

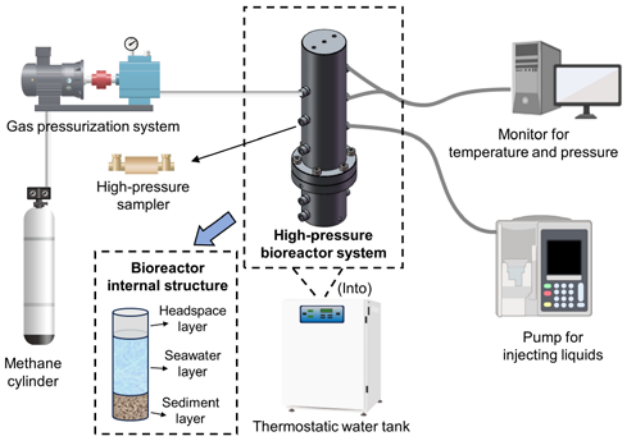

Fig. 1 The high-pressure bioreactor system

2.3 Activation of the sediment at ambient pressure

All manipulations were carried out under an anoxic atmosphere of N_2 using an anoxic glove box (LAI–3DT, Longyue Techno Co., Ltd, Shanghai). The original sediment was 2 times diluted with artificial seawater medium. Every liter of the basal medium consisted of NaCl 9.88 g, $MgCl_2{\cdot}6H_2O$ 2.12 g, $CaCl_2{\cdot}2H_2O$ 0.55 g, $MgSO_4{\cdot}7H_2O$ 2.55 g, NH_4Cl 3.93 g, KH_2PO_4 2 g, KCl 0.23 g, KBr 0.03 g, a bicarbonate solution 30 mL, a trace element solution 1 mL, a vitamin mixture solution 1 mL, a thiamine solution 1 mL, and a vitamin B_{12} solution 1 mL. The pH of the medium was adjusted to 6.8 by adding sulfuric acid. The headspace was flushed and filled with methane at 8 MPa system pressure. Continuous incubation was performed in the dark closed system at 15°C and 8°C. Four experimental groups were designed based on different temperatures and sulfate concentrations as Table 1. In addition, Na_2SO_4 (15 mM) was used as the sulfate supply substance in the system. The period of each set of experiments was 50 days. At the end of each period of the experiment, the activated slurry was then flushed with methane gas to remove accumulated sulfide and further diluted with fresh medium up to 4 times dilution. Sulfuric acid was added to adjust the pH back to 7. During each period, layers of headspace, seawater, and sediment in the system were sampled every 10 days. The samples of gas, seawater, sediment, and pore water were immediately subjected to geochemical analysis.

Table 1 Experimental design showing the incubation conditions

Incubation group	Temperatures (°C)	Sulfate addition (mM)	Time (day)
H1	15	0	50
H2	15	15	50
C1	8	0	50
C2	8	15	50

2.4 Geochemical analysis

The concentration of sulfate (SO_4^{2-}) was detected using ion chromatography (Thermo Fisher AQ-1200, Waltham, MA, USA) operating at 30°C. An AS11-HC column was used at a flow rate of 1 mL/min. The ADRS600 suppressor current was set at 120 mA, and the sample test was conducted according to the manufacturer's instructions. The measurement of product sulfide by methylene blue method using a spectrophotometer (HACH DR1900, Loveland, USA).

The headspace and dissolved gas samples collected from the bioreactor were quantified by headspace gas chromatography [12]. After gas equilibration, 0.5 mL of headspace gas was injected into a gas chromatograph (GC, Thermo Fisher TRACE1300, Waltham, MA, USA) with a flame-ionization detector. High-purity helium (99.99%) was used as the carrier gas at a flow rate of 30 mL/min. The precision of the analytical method was ± 2.5%.

2.5 Calculation

The values of the gas components of CH_4 and CO_2 in this sample were measured by gas chromatograph. The content of the gas in the headspace layer of the bioreactor system was calculated using the above values by equation (1). The content of the dissolved gas in the seawater layer of the system was calculated by equation (2) as well as by Bunsen's coefficient β under the given conditions. In addition, the content of the dissolved gas in the sediment layer of the system was calculated using equation (2) with the water content of the sediment. In the calculation of the methane oxidation rate, it was hypothesized that the AOM can be modeled as a first-order kinetic process during the exponential oxidation phase [12]. The first-order kinetic constant, i.e., the oxidation rate constant k_{ox}, can be calculated using equation (3). The methane oxidation rate r_{ox} of the reaction system can be calculated using the constant and then equation (4).

$$n(CH_4)_{hs} = \frac{pCH_{4\,hs} \times V_{hs} \times P_{hs}}{R(273.15+T)} \quad (1)$$

where $n(CH_4)_{hs}$ is the molar amount of methane in the headspace; pCH_{4hs} is the partial pressure of methane gas; V_{hs} is the volume of the headspace; P_{hs} is the headspace pressure; R is the ideal gas constant; and T is the experimental temperature.

$$n(CH_4)_w = \beta \frac{pCH_{4\,hs} \times V_{gas} \times (V_w / V_{hs})}{R(273.15+T)} \quad (2)$$

where $n(CH_4)_w$ is the molar amount of methane in the dissolved state; pCH_{4hs} is the partial pressure of methane gas; V_{gas} is the volume of headspace; V_w is the volume of water; V_{hs} is the volume of headspace; R is the ideal gas constant; T is the experimental temperature; and β is the Bunsen's coefficient.

$$\ln\left(\frac{n(CH_4)_{total,ti}}{n(CH_4)_{total,ti-1}}\right) = -k_{ox,ppm} \times ti_{-(i-1)} \quad (3)$$

where $n(CH_4)_{total}$, t_i is the total molar content of methane during a certain reaction time; t_i is the reaction time; k_{ox} is the methane oxidation rate constant, which is the negative slope of the linear regression between $\ln(nCH_4)$ and time (t_i). Positive values of k_{ox} indicate a decrease in methane concentration, and negative values of k_{ox} indicate an increase.

$$r_{ox} = k_{ox} \times n(CH_4)_{total} / V \quad (4)$$

where r_{ox} is the methane oxidation rate; k_{ox} is the oxidation rate constant; $n(CH_4)_{total}$ is the total molar amount of methane; V is the volume of the reaction system.

3. RESULTS AND DISCUSSION

3.1 The effect of temperature on the AOM process

The results in this paper have demonstrated that when the temperature was decreased, the AOM process was inhibited (Fig. 2). In the headspace layer, decreasing the temperature reduced the consumption of CH_4 and the production of CO_2. Due to the nature of the gases in the system, the gas content in the headspace layer can reflect the gas content of the entire system. In addition, the AOM rates were significantly affected by temperature regardless of the presence or absence of increased sulfate (Fig. 3). From the reaction of AOM, the content of the product CO_2 did not show a significant increase at a low temperature (8°C). Differences in the SR-AOM process due to temperature variations were evident in the seawater and sediment layers, and were mainly reflected in changes in the content of sulfide and sulfate. Sulfate in the seawater layer did not change

obviously at 8°C, while it was apparently consumed at 15°C. Sulfate was slightly increased in the sediment layer, probably due to the mass transfer by seawater. The production of sulfide in the sediment layer was significantly inhibited at the low temperature. With respect to dissolved gases, the content of CH_4 and CO_2 in the seawater and sediment layers showed a similar trend at different temperatures, which may be related to its dissolution at high pressure (8 MPa). It was evident that sulfate reduction was significantly inhibited at a low temperature. The sulfate reduction process was sensitive to temperature, which affected the SR-AOM process in collaboration with ANME archaea and sulfate-reducing bacteria. Thus, temperature affected the AOM process by inhibiting the reaction of sulfate reduction.

3.2 The effect of sulfate concentration on the AOM process

We simulated sulfate supply with a fed-batch mode of the bioreactor, and found that the AOM process was stimulated when sulfate concentration increased in the system (Fig. 2). In the headspace layer, the magnitude of CH_4 consumption was increased by increasing sulfate concentration. The rate of AOM supplemented with sulfate was higher than that of AOM without added sulfate, regardless of temperature (Fig. 3). The effect of sulfate on the SR-AOM process was obvious in the seawater layer at the higher temperature (15°C), mainly in terms of changes in the content of sulfide and sulfate. Especially in the seawater layer, sulfate concentration was drastically reduced, while the content of the product sulfide (S^{2-}) was significantly increased. In contrast, the concentrations of sulfide and sulfate both in the layer of seawater and sediment did not change significantly at the low temperatures (8°C), even after sulfate supplementation. It was clear that the sulfate reduction process was significantly inhibited by the low temperature. With respect to dissolved gases, it was interesting to note that the production of CO_2 was decreased after sulfate supplementation, which may be related to the decoupling of the AOM and SR processes. The increased sulfate concentration in the system may stimulate the sulfur cycling process. In the environment of high sulfate concentrations, sulfur-nutrient-related bacteria grew rapidly thus enhancing the SR process. Hence, high concentrations of sulfate affected the methane oxidation through the decoupling of the SR-AOM process.

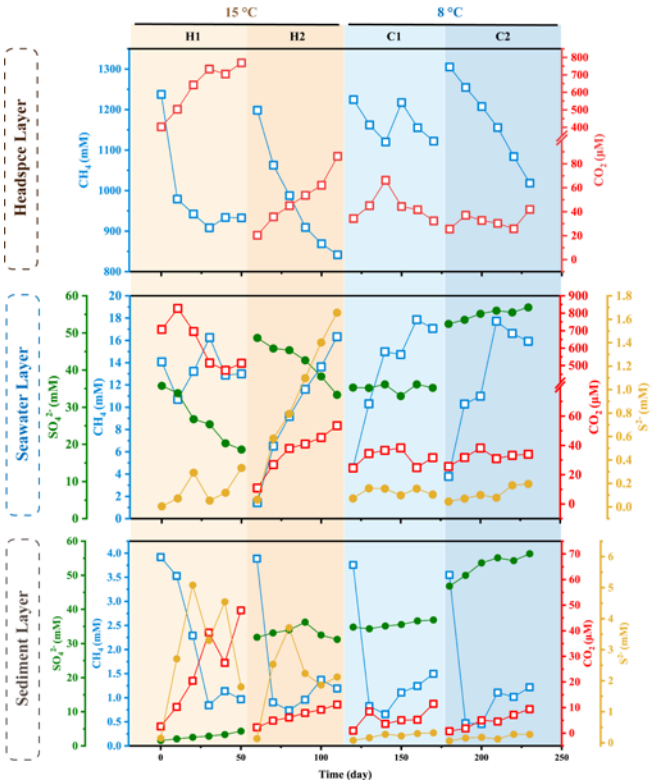

Fig. 2 The AOM process under different conditions of temperature and sulfate concentration

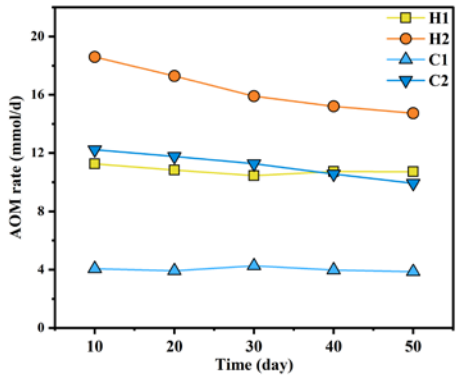

Fig. 3 The variation of the AOM rate at different temperature and sulfate concentration

3.3 The compound effect of sulfate concentration on the AOM process

In this study, the results showed that both temperature and increased sulfate concentration affected the AOM process. There may be a superimposed effect under the coexisting conditions in varying temperature and sulfate concentration, as demonstrated by the fact that the AOM activity was stimulated significantly under the conditions of high temperature and high sulfate concentration. At the temperature of 15°C, the system reached its highest AOM rate with the sulfate addition (Fig. 3). At that

condition, the content of CH_4, CO_2, SO_4^{2-}, and S^{2-} in the system all changed to a greater extent compared to other conditions (Fig. 2). Conversely, the AOM rate was decreased due to the low temperature, while the rate was recovered to a high level after sulfate addition. This was probably due to the decrease in microbial activity at a low temperature, while the increased sulfate stimulated the sulfur cycle thereby enhancing the SR process. Therefore, both temperature and sulfate concentration have important effects on the AOM process.

3.4 Implications for the calculation of global methane balances

Globally, different conditions of temperature and sulfate concentration represent distinct habitats in the cold seep. Sulphate is supplemented by the upper water column, and its concentration varies in different sediment depths and areas. The temperature difference is mainly reflected in the water depth and geographical latitude of the cold seep habitats. This usually explains the differences in AOM processes in the different seep habitats where in situ surveys are conducted. This study can provide a reference basis for the assessment of AOM processes in those distinct habitats. The rates of methane oxidation should be at high levels in the environments with high temperatures (at low latitudes or in habitats with small water depths) and high sulfate concentrations (at the sediment surface or in habitats close to land). The fine-scale assessment of methane budgets will provide important support for the future accounting of global carbon emissions.

4. CONCLUSIONS

Anaerobic oxidation of methane as an ecological barrier in the deep sea varies across cold seep habitats. We simulated the habitat differences in sulfate and temperature using a high-pressure bioreactor system. The seep sediment was incubated in vitro using a fed-batch mode to assess differences in the AOM rates and the geochemical processes. The SR-AOM process was found to be significantly affected by increased temperature (15°C). The AOM activity was increased by sulfate supply (+15 mM), even at a low temperature (8°C). These findings provide a new insight into the methane budgets in cold seeps for the future accounting of global carbon emissions.

ACKNOWLEDGEMENT

We are grateful to the crew of the “Kexue” expedition vessel and ROV Haima team for their assistance in collecting the sediment samples. This work was financially supported by the National Key Research and Development Program of China (2021YFF0502300), the National Natural Science Foundation of China (41890850, 42022046, 42227803, L2124013), the Guangdong Natural Resources Foundation, (GDNRC[2022]45, GDNRC[2023]30), and the PI project of Southern Marine Science and Engineering Guangdong Laboratory (Guangzhou) (GML20190609 and GML2022009).

REFERENCE

[1] Zhou T. New physical science behind climate change: What does IPCC AR6 tell us? The Innovation. 2021;2:100173.

[2] Wang Y, Feng J-C, Li X-S, Zhang Y, Han H. Experimental Investigation on Sediment Deformation during Gas Hydrate Decomposition for Different Hydrate Reservoir Types. Energy Procedia. 2017;142:4110-6.

[3] Feng J-C, Yan J, Wang Y, Yang Z, Zhang S, Liang S, et al. Methane mitigation: Learning from the natural marine environment. The Innovation. 2022;3:100297.

[4] Liu J, Robinson C, Wallace D, Legendre L, Jiao N. Ocean negative carbon emissions: A new UN Decade program. The Innovation. 2022;3:100302.

[5] Feng J-C, Yang Z, Zhou W, Feng X, Wei F, Li B, et al. Interactions of Microplastics and Methane Seepage in the Deep-Sea Environment. Engineering. 2022.

[6] Barnes RO, Goldberg ED. Methane production and consumption in anoxic marine sediments. Geology. 1976;4:297-300.

[7] Boetius A, Ravenschlag K, Schubert CJ, Rickert D, Widdel F, Gieseke A, et al. A marine microbial consortium apparently mediating anaerobic oxidation of methane. Nature. 2000;407:623-6.

[8] Knittel K, Boetius A. Anaerobic Oxidation of Methane: Progress with an Unknown Process. Annual Review of Microbiology. 2009;63:311-34.

[9] Gao Y, Wang Y, Lee H-S, Jin P. Significance of anaerobic oxidation of methane (AOM) in mitigating methane emission from major natural and anthropogenic sources: a review of AOM rates in recent publications. Environmental Science: Advances. 2022;1:401-25.

[10] Ferré B, Jansson PG, Moser M, Serov P, Portnov A, Graves CA, et al. Reduced methane seepage from Arctic

sediments during cold bottom-water conditions. Nature Geoscience. 2020;13:144-8.
[11] Yu H, Skennerton CT, Chadwick GL, Leu AO, Aoki M, Tyson GW, et al. Sulfate differentially stimulates but is not respired by diverse anaerobic methanotrophic archaea. The ISME Journal. 2022;16:168-77.
[12] Magen C, Lapham LL, Pohlman JW, Marshall K, Bosman S, Casso M, et al. A simple headspace equilibration method for measuring dissolved methane. Limnology and Oceanography: Methods. 2014;12:637-50.